LEGO-Inspired Electrically-Actuated Microfluidics for On-Chip Protein Crystallization and *In-Situ* X-ray Crystallography

Sarthak Saha,[1,†] Logan Chen,[1,†] Gabrielle R. Budziszewski,[2,3] Sara Koprek,[1] Kaleb Seifert,[4] Aina Cohen,[5] Silvia Russi,[5] Sarah E.J. Bowman,[2,3] Sarah L. Perry[1,*]

[1] Department of Chemical and Biomolecular Engineering, University of Massachusetts Amherst, Amherst, MA 01003, USA

[2] Department of Biochemistry, Jacobs School of Medicine and Biomedical Sciences at The State University at Buffalo, Buffalo, NY 14023, USA

[3] University at Buffalo Hauptman Woodward Research Institute, Buffalo, NY,14203, USA

[4] Department of Biomedical Engineering, University of Massachusetts Amherst, Amherst, MA 01003, USA

[5] SLAC National Accelerator Laboratory, Menlo Park, CA 94025, USA

[†] Authors contributed equally

[*] Correspondence email: perrys@engin.umass.edu

Table S1. Crystallographic statistics for data obtained at room temperature for Rubrerythrin grown in LEAP-X and traditional vapour diffusion.

	Rubrerythrin (LEAP-X, merged from two crystal)	Rubrerythrin (Vapour Diffusion harvested, Single crystal)
Data collection		
Space group	R3 PDB 9P19	R3 PDB 9P1A
Cell dimensions		
a, b, c (Å)	203.4, 203.4, 71.08	203.36, 203.36, 69.87
α, β, γ (°)	90, 90, 120	90, 90, 120
Resolution (Å)	30.15-1.96 (1.99-1.96)	29.35-1.93 (1.97-1.93)
R_{meas}	0.12 (1.4)	0.26 (4.3)
Mean I/σI	5.8 (0.4)	5.2 (0.6)
Completeness (%)	95.8 (94.5)	100.0 (100.0)
$CC_{1/2}$	0.945 (0.257)	0.990 (0.197)
CC*	0.986 (0.639)	0.997 (0.574)
Refinement		
Resolution (Å)	30.15-1.96	29.35-1.93
Unique reflections	12677	154394
R_{work} / R_{free} (%)	16.67/21.27	18.50/22.27
Ramachadran plot		
In preferred regions (%)	97.57	97.32
Outliers (%)	0.00	0.00
r.m.s. deviations		
Bond lengths (Å)	0.01	0.01
Bond angles (°)	0.976	1.032

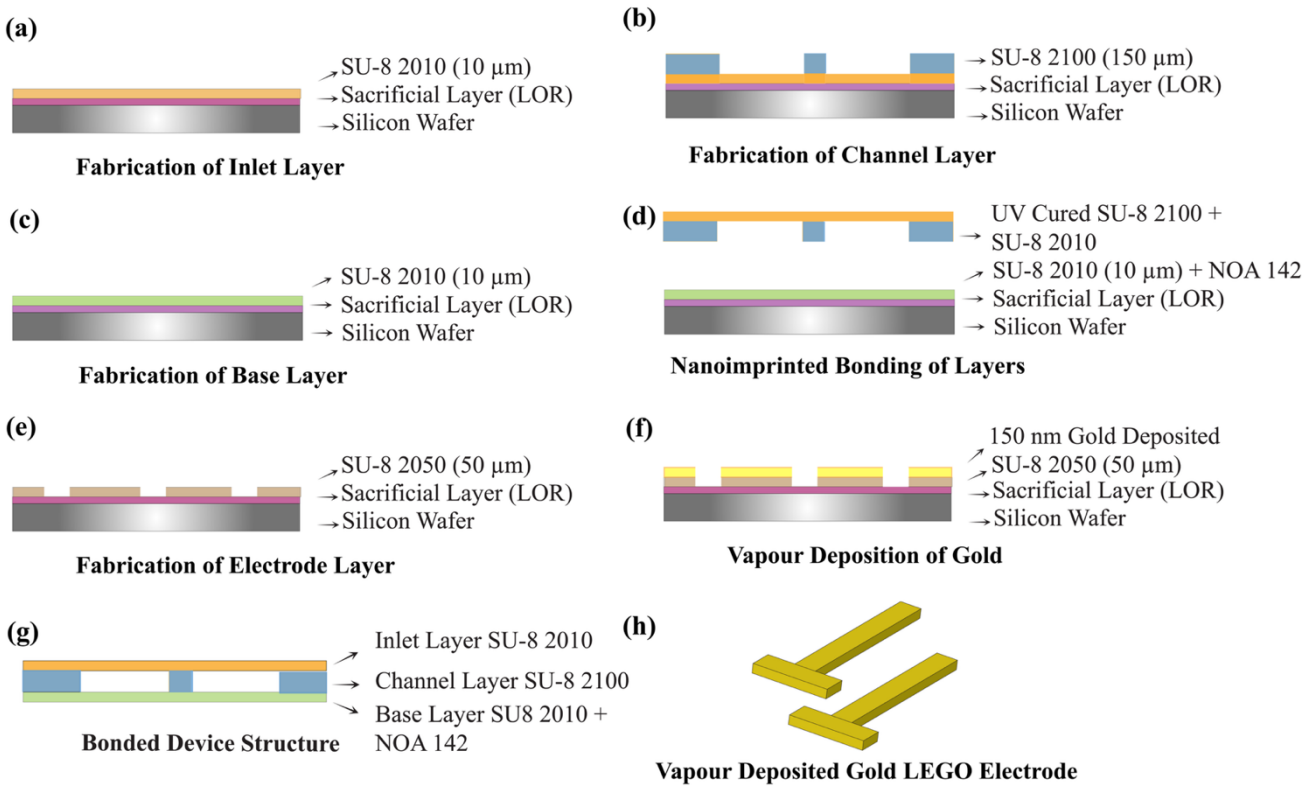

Figure S1. Schematic **(a)-(d)** showing step-by-step fabrication of LEAP-X using photolithography and nanoimprinting and **(e)-(f)** showing the fabrication of gold LEGO electrode (GLE), **(g)** side view of the bonded device and **(h)** schematic of the GLE.

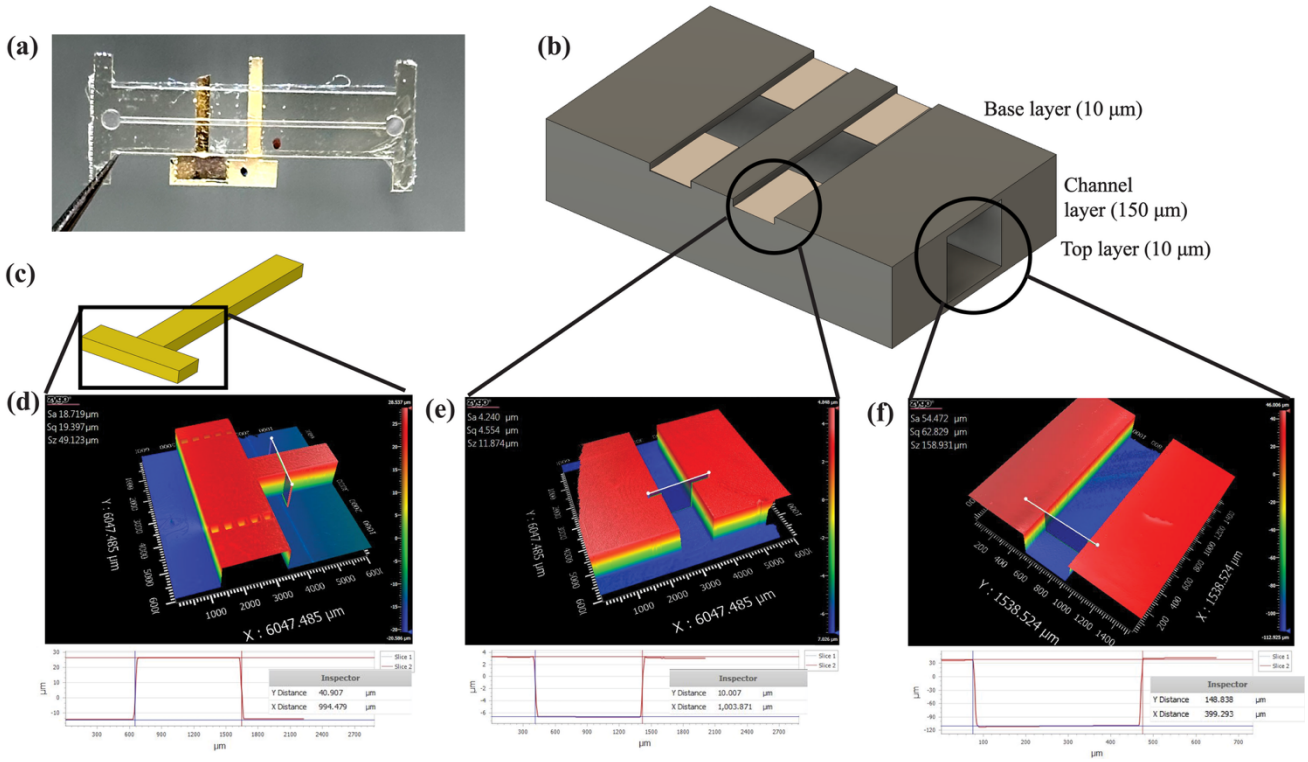

Figure S2. (a) Optical micrographs of the assembled LEAP-X **(b)** 3D model of the valving area; and **(c)** gold electrodes. Panels **(d–f)** show optical profilometry data (3D images and 2D cross-sections) of the electrode, the electrode gaps in the bottom layer, and the open channel depth prior to nanoimprinting, respectively.

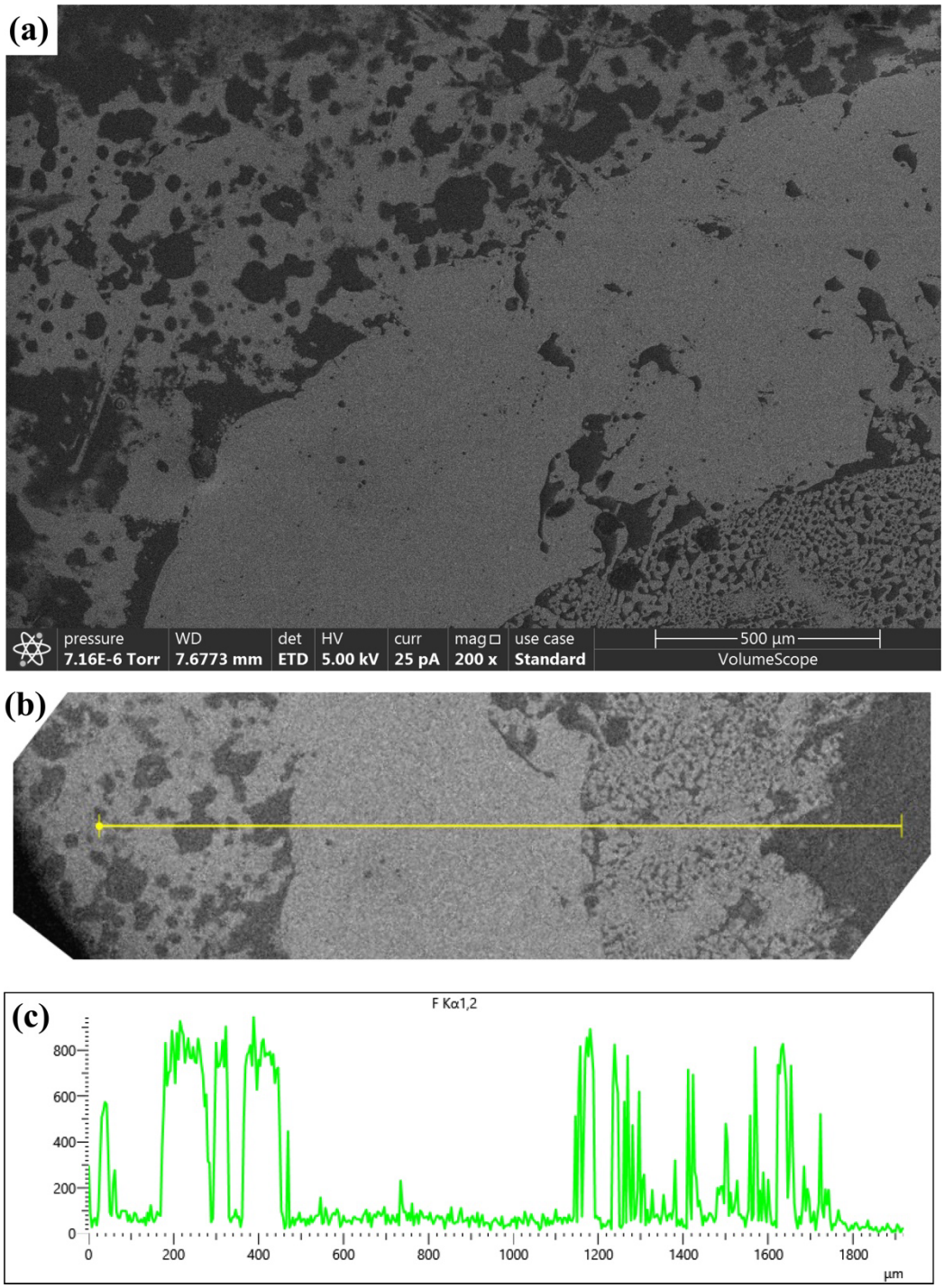

Figure S3. (a) Scanning electron micrograph of the silane deposited gold electrode showing the removal of silane in a coffee ring manner. **(b)** A line trace of the same image and **(c)** the corresponding fluorine signal from energy dispersive X-ray spectroscopy (EDS).

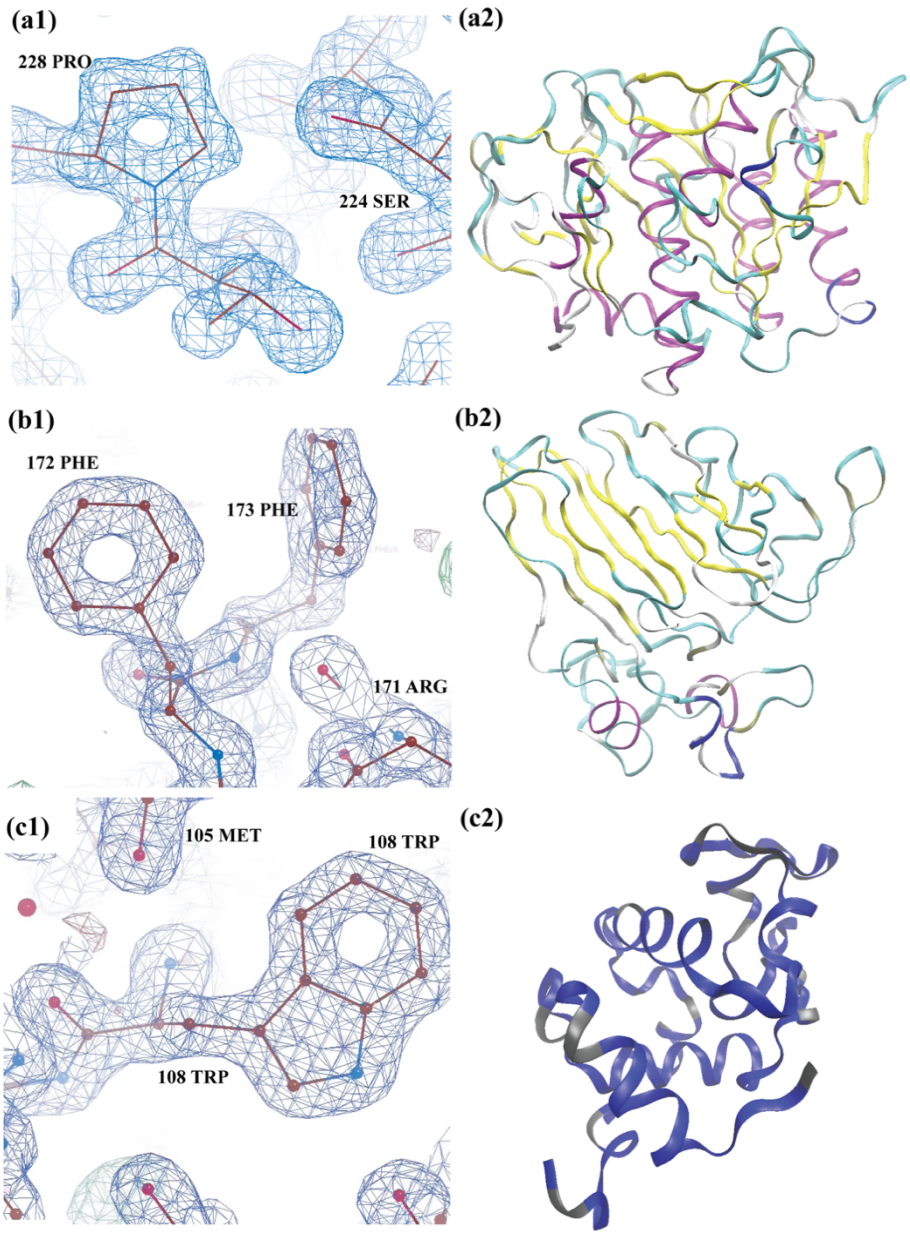

Figure S4. The representative 2Fo-Fc map contoured at σ = 1.1 and the corresponding structure of **(a)** proteinase K, **(b)** thaumatin, and **(c)** lysozyme.

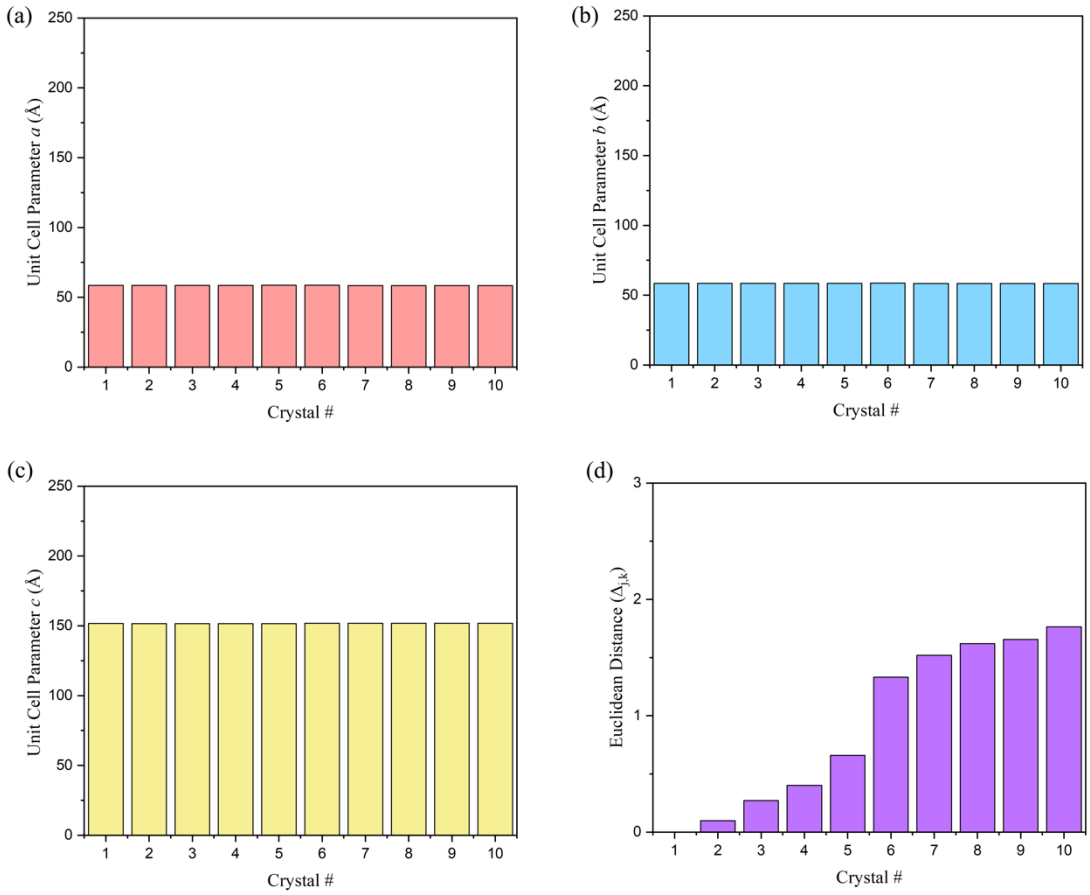

Figure S5. (a)-(c) Plot of the variation in the corresponding unit cell parameter across the 10 crystals of thaumatin analyzed, and **(d)** a plot of the standard Euclidian distance $\Delta_{j,k}$ vs. crystal, showing the variation in the unit cell parameters.

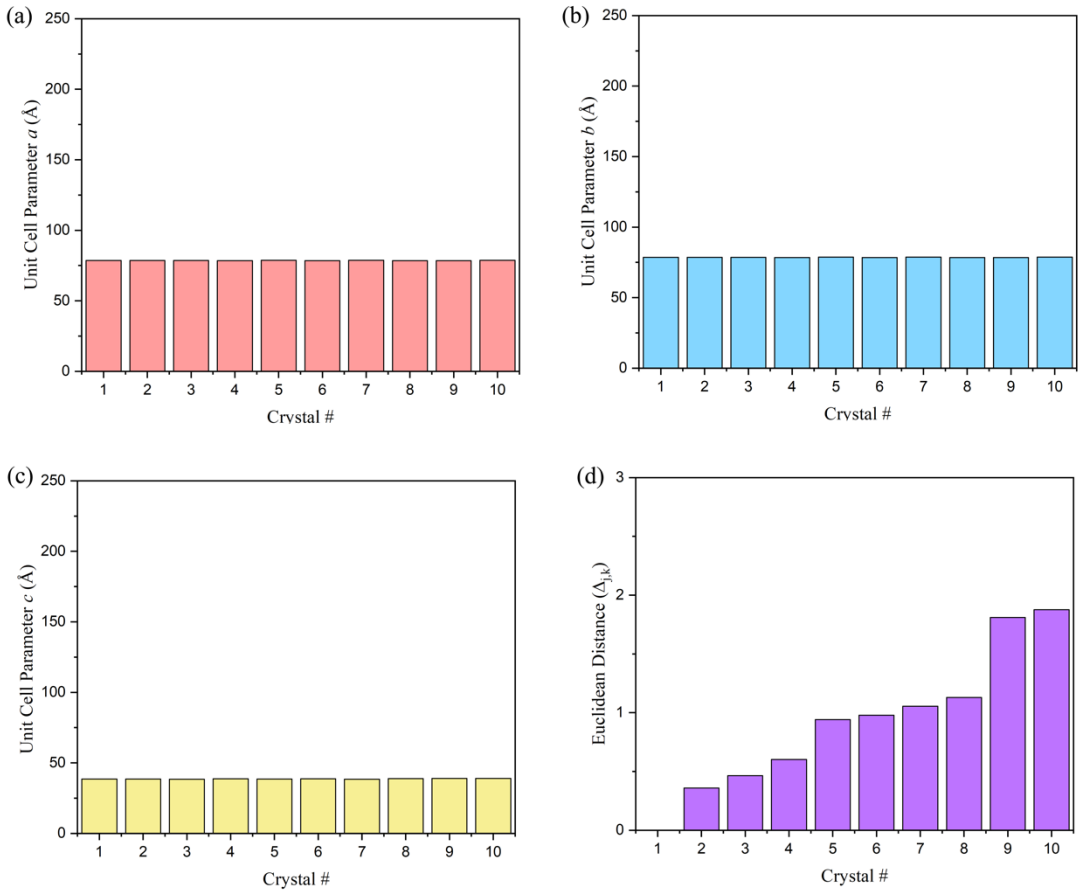

Figure S6. (a)-(c) Plot of the variation in the corresponding unit cell parameter across the 10 crystals of lysozyme analyzed, and **(d)** a plot of the standard Euclidian distance $\Delta_{j,k}$ vs. crystal, showing the variation in the unit cell parameters.

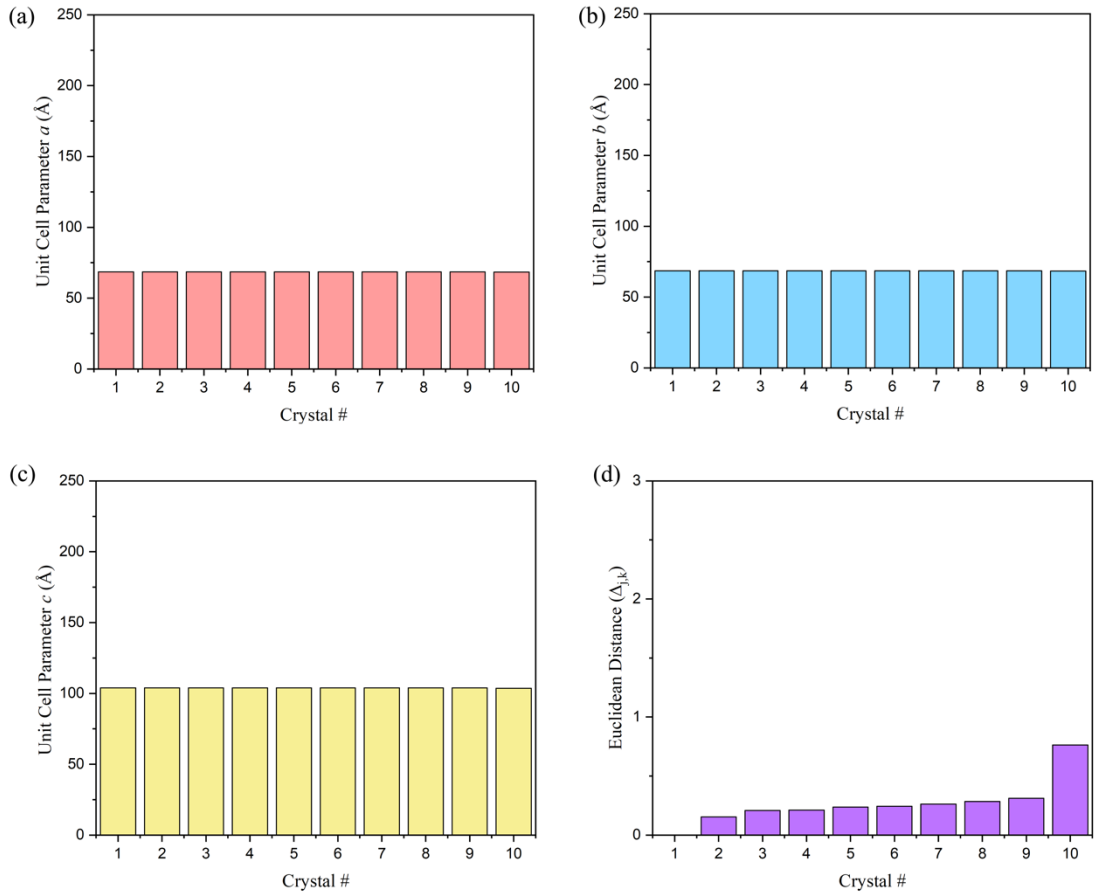

Figure S7. (a)-(c) Plot of the variation in the corresponding unit cell parameter across the 10 crystals of proteinase K analyzed, and **(d)** a plot of the standard Euclidian distance $\Delta_{j,k}$ vs. crystal, showing the variation in the unit cell parameters.

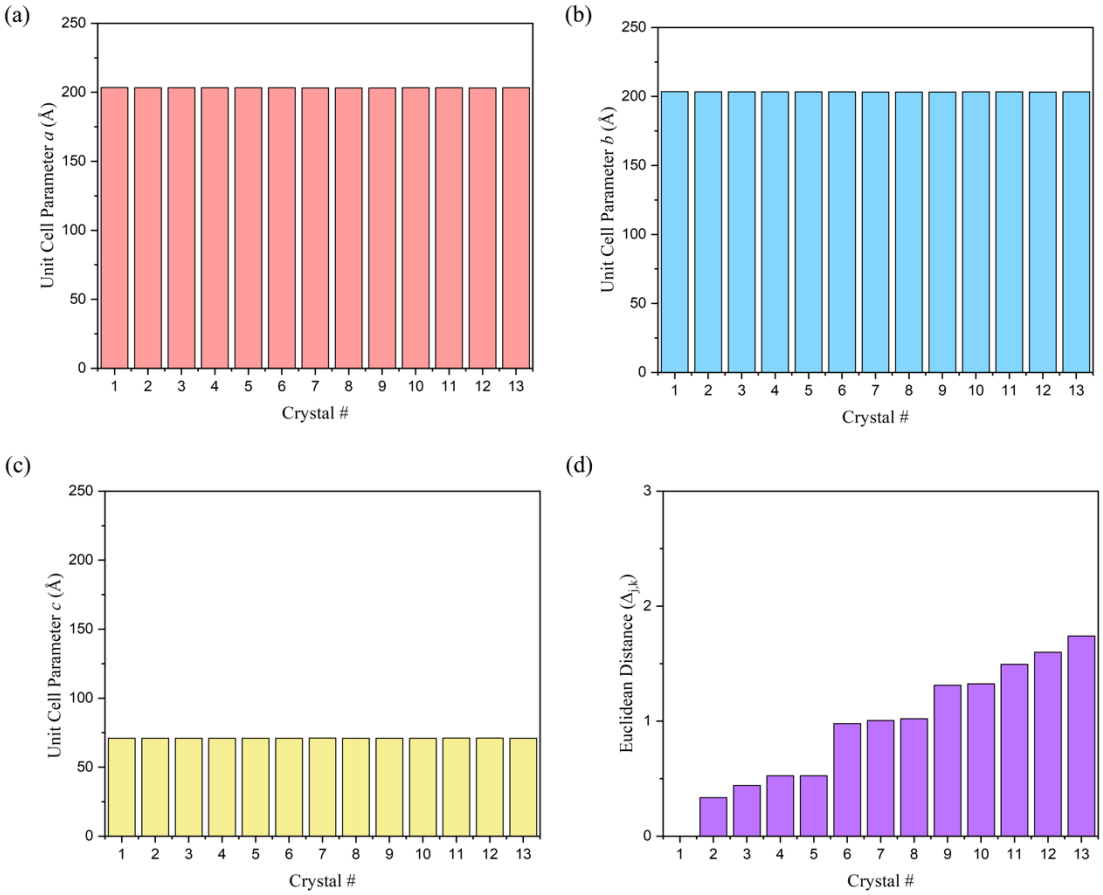

Figure S8. (a)-(c) Plot of the variation in the corresponding unit cell parameter across the 13 crystals of rubrerythrin analyzed, and **(d)** a plot of the standard Euclidian distance $\Delta_{j,k}$ vs. crystal, showing the variation in the unit cell parameters.